



Solvatochromic, acid–base features and time effect of some azo dyes derived from 1,3-benzothiazol-2-ylacetonitrile: Experimental and semiempirical investigations

Y.H. Ebead^{a,*}, M.A. Selim^a, S.A. Ibrahim^b

^a South Valley University, Faculty of Science, Chemistry Department, 83523 Qena, Egypt

^b Assiut University, Faculty of Science, Chemistry Department, 71516 Assiut, Egypt

ARTICLE INFO

Article history:

Received 26 October 2009

Accepted 19 November 2009

Keywords:

Azo dyes

Solvatochromism

Acid–base properties

Semiempirical calculations

Time effect

ABSTRACT

The solvatochromism and other spectroscopic properties of seven azo dyes were studied, with a particular respect to the role of the solvent basicity, and interpreted with the aid of experimental findings and semiempirical data. The electronic absorption spectra of the dyes examined in different solvents combined with theoretical calculations showed that most of the investigated compounds coexist in the hydrazone and/or azo-enamine-common anion equilibrium or in the solely anionic form depending upon the nature of the solvent employed. These interesting features open up possibilities for the use of these compounds in analytical chemistry as acid–base indicators. Furthermore, both of intermolecular and intramolecular charge transfer equilibria have been reflected by experimental absorption spectra of compounds **4** and **5**. The enthalpies of formation predicted at PM6 (COSMO) and PM6/CI (COSMO) for the ground (S_0) and excited (S_1) states, respectively have been successfully used for the explanation of the observed bathchromic shift in non-polar solvents. The effect of time on the longer wavelength visible band of compound **7** has been thoroughly investigated.

© 2009 Elsevier B.V. All rights reserved.

1. Introduction

Electronic absorption spectroscopy is one of the most powerful tools available to chemists and widely used for the identification and determination of myriad inorganic and organic species, particularly for determining environmental pollutants [1,2]. Consequently, it is probably more widely used in chemical and clinical laboratories – because many substances can be selectively converted into a color derivative – throughout the world than any other single procedure [3]. However, synthesis of new azo compounds and studying their physicochemical properties are important subjects due to their fundamental role in biological, pharmaceutical and colorimetric chemosensors for metal ions [4–9]. Of particular interest are their widespread commercial applications in a textile dyeing industries as well as food, cosmetic and ink-jet printers [10,11]. Nevertheless, azo dyes are not renowned for recalcitrant to biodegradation and consequently they contribute to mutagenic activity of ground and surface waters pollution [12,13]. Considering their significant biological activity, pharmacological and physicochemical properties, azo dyes are extremely important. In a broader sense, the azo dyes constitute the largest group of all the synthetic

colorants [10,14,15]. Recently, the demand for such group of compounds especially those having sufficient large non-linear optics (NLO) have increased as a result of several new technological applications that have been found [16–18]. Furthermore, azo dyes have received considerable attention in the field of solvatochromic studies and in the design of polarity scale [19–21]. It is well-known that benzothiazole derivatives show a broad spectrum of biological activities [22–24]. Additionally, benzothiazole and its derivatives were investigated in azo push–pull systems [25]. In continuation of our earlier work on azo and other biologically active compounds [26–29], the present work focuses on the synthesis, spectroscopic properties of some novel azo dyes derived from 1,3-benzothiazol-2-ylacetonitrile using UV–vis and semiempirical molecular orbital PM3, PM6 methods. Furthermore, the effect of time on the low energy band of compound **7** appearing in the basic solvent (DMF) has been also investigated. A wide variety of organic solvents have been employed, aiming to evaluate which tautomeric form of these compounds is spectroscopically active, considering their possible applications as indicators or spectral probes.

2. Experimental

2.1. Synthesis of the azo compounds 1–7 (Scheme 1)

The azo compounds under investigation were prepared according to the procedure previously described in the literature [30,31].

* Corresponding author. Tel.: +20 108928365; fax: +20 96/5213383.

E-mail address: ebeadhassan88@yahoo.com (Y.H. Ebead).

Thus, to an ice cooled stirred solution of the proper primary aromatic amine (0.01 mol) dissolved in diluted HCl a cold solution of NaNO₂ (0.01 mol) was added gradually with stirring for 20 min. To a solution of 1,3-benzothiazole-2-ylacetonitrile (0.01 mol) [32] in ethanol in the presence of sodium acetate (0.01 mol), a solution of diazotized amine was added dropwise with vigorous stirring at 0–5 °C for 35 min. After the addition, stirring was continued for 1 h and the obtained precipitate was filtered off and washed with water and cold ethanol. The solid products were recrystallized from ethanol and dried in vacuo over silica gel. The chemical structures of compounds were assigned on the basis of their elemental analysis and spectral data (Table 1).

2.2. Measurements

The chemical composition of the products was proved by elemental analysis using Carlo-Erba (model EAGER 200) instrument. Melting points were determined by Electro-thermal melting point apparatus. Spectral measurements in the UV and visible regions were recorded on a Shimaduz 2401 PC spectrophotometer within the wavelength range 200–700 nm using 1-cm matched quartz cell. ¹H NMR (DMSO-d₆) spectra were taken on a Varian Mercury VX-300 MHz spectrometer. All solvents (methanol, ethanol, acetone, acetonitrile, carbon tetrachloride, chloroform, methylenechloride, dimethylsulfoxide and dimethylformamide) used in this investigation were analytically pure or spectroscopic grade and were used as purchased. Infrared spectra of the solids were performed on a FT-IR Bruker Vector 22 using the KBr technique. All the measurements were carried out at room temperature (25 °C).

2.3. Quantum chemical calculations

The fully geometry optimization of the isolated molecules **1–7** (Scheme 1) in ground (S₀) and first excited (S₁) states were optimized using the semiempirical PM6 and PM6/CI methods [33]. From which some physicochemical and structural parameters in gaseous phase for each tautomer were estimated. Solvent effects on tautomers were also investigated using PM6 (COSMO) model [33] as implemented in MOPAC 2007. PM3 method was employed for comparison when it was necessary [34]. The geometry data were obtained from MOPAC 2007—free license on internet [35]. The wavelengths of the electronic transitions in absorption spectra were calculated at AM1 with a 10 × 10 CI singly excited matrix [36]. Heats of formation, dipole moments and other parameters were extracted directly from the data files following the geometry optimizations. All calculations were done on a Pentium IV PC computer.

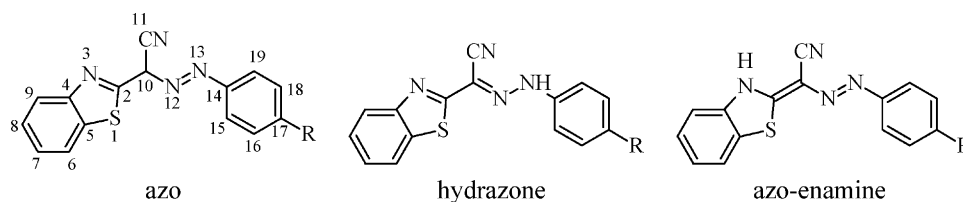
3. Results and discussion

3.1. Structural and physicochemical features of the molecules in the ground and excited states

Three different structures could be written corresponding to the molecular composition of each compound namely, azo, hydrazone and azo-enamine (Scheme 1). This is due to the migration of the hydrogen atom attached to C₁₀ to the benzothiazole nitrogen atom or to N₁₃. A further tautomeric structure is also possible in the case of compound **7** (R=OH) as a result of transfer of the phenolic OH proton to N₁₂. The latter tautomer is excluded from our discussion due to its high heat of formation. Azo, hydrazone and azo-enamine as well as the anionic forms have been geometrically optimized in the gaseous phase and in different media using PM6 and PM6 (COSMO), respectively. PM6 which has been recently released as a modification on NDDO formalism gave satisfactory estimates of

Table 1
Microchemical analysis data, melting points, color, IR and ¹H NMR spectra of the synthesized compounds.

Comp.	Formula	m.p. (°C)	Color	% Calculated (found)				IR ν (cm ⁻¹)		¹ H NMR (ppm)
				C	H	N	S	ν (NH)	ν (C≡N)	
1	C ₁₅ H ₁₀ N ₄ S	155–157	Green yellow	64.67 (64.10)	3.59 (3.48)	20.12 (19.87)	11.50 (11.77)	3449	2217	12.22 (s, 1H, NH), 7.12–8.09 (m, 9H, Ar-H)
2	C ₁₆ H ₁₂ N ₄ S	182–184	Dark yellow	65.67 (65.29)	4.10 (3.80)	19.15 (19.11)	10.95 (11.07)	3462	2216	12.16 (s, 1H, NH), 7.21–8.19 (m, 8H, Ar-H), 2.29 (s, 3H, CH ₃)
3	C ₁₆ H ₁₂ N ₄ O ₅	162–164	Orange	62.26 (61.75)	3.89 (3.50)	18.16 (18.17)	10.38 (10.32)	3456	2217	12.17 (s, 1H, NH), 7.00–8.07 (m, 8H, Ar-H), 3.80 (s, 3H, OCH ₃)
4	C ₁₆ H ₁₀ N ₄ O ₂ S	269–271	Yellow	59.56 (59.16)	3.10 (3.43)	17.37 (17.16)	9.93 (9.80)	3456	2223	13.80 (s, 1H, COOH), 12.15 (s, 1H, NH), 7.00–8.20 (m, 8H, Ar-H)
5	C ₁₅ H ₈ N ₆ O ₂ S	237–239	Dark yellow	55.67 (55.20)	2.78 (3.08)	21.65 (21.40)	9.89 (9.37)	3483	2230	12.60 (s, 1H, NH), 7.48–8.33 (m, 8H, Ar-H)
6	C ₁₅ H ₉ ClN ₄ S	174–176	Yellow	57.55 (57.17)	2.88 (2.77)	17.90 (17.93)	10.23 (10.12)	3436	2230	12.27 (s, 1H, NH), 7.45–8.10 (m, 8H, Ar-H)
7	C ₁₅ H ₁₀ N ₄ O ₅	221–223	Brown	61.16 (60.79)	3.39 (3.07)	19.03 (19.07)	10.87 (10.86)	3469	2209	14.40 (s, 1H, OH), 12.12 (s, 1H, NH), 6.81–8.25 (m, 8H, Ar-H)



Scheme 1. The compounds investigated with the number of atoms indicated: **1**–1,3-benzothiazol-2-yl[(E)-phenyldiazenyl]acetonitrile; **2**–1,3-benzothiazol-2-yl[(E)-(4-methylphenyl)diazenyl]acetonitrile (p-CH₃); **3**–1,3-benzothiazol-2-yl[(E)-(4-methoxyphenyl)diazenyl]acetonitrile (p-OCH₃); **4**–1,3-benzothiazol-2-yl[(E)-(4-carboxylphenyl)diazenyl]acetonitrile (p-COOH); **5**–1,3-benzothiazol-2-yl[(E)-(4-nitrophenyl)diazenyl]acetonitrile (p-NO₂); **6**–1,3-benzothiazol-2-yl[(E)-(4-chlorophenyl)diazenyl]acetonitrile (p-Cl); **7**–1,3-benzothiazol-2-yl[(E)-(4-hydroxyphenyl)diazenyl]acetonitrile (p-OH).

several molecular and physical properties such as heats of formation and electronic dipole polarizability and many other various properties [37,38]. Analysis of the optimized molecular geometries reveals that the azo and hydrazone tautomers are essentially non-planar in the ground and excited electronic states since a significant torsion angles are detected between the plane of the azo linkage and the carbons C₂ and C₁₀ (Fig. 1, Table 2). In contrast, our calculations on the other forms considered here gave structures in which the heterocyclic moiety is essentially coplanar with the rest of the molecule (Table 2).

In the light of our data obtained from PM6 in the gaseous phase, the azo tautomers were found to be less thermodynamically stable than the other ones (Table 2). Moreover, the energy difference between both hydrazone and azo-enamine tautomers in ΔH_f of each dye was ranging from 1 to 2 kcal/mol. The highest energy difference – 3 kcal/mol – was found only for compound **5** and the calculated values of heats of formation of various forms in non-aqueous media predicted are presented in Table 3. Calculations combining COSMO in semiempirical calculations demonstrate that the inclusion of a continuum dielectric representing a particular solvent provides lower values of enthalpies of formation in respect with the ones estimated at the gaseous phase. Furthermore, hydrazone and azo-enamine tautomers are still thermodynamically preferred compared to the corresponding azo tautomer and can coexist in equilibrium as a consequence. It is worthwhile men-

tioning that the differences in the enthalpies of formation of the relevant excited and ground state forms remain comparable and only slightly affected by the medium properties. In addition, the thermodynamically preferred tautomers in the ground state are also favorable in the excited state for all compounds investigated.

Changes in the dipole moment as a result of electronic excitation ($\mu_{S_1} - \mu_{S_0}$) for each tautomeric form are quite clear. The dipole moment changes accompanying electronic excitation in the case of azo-enamine forms are not very high but always negative, though they are mainly positive in the hydrazone tautomers. This implies that the positions of the long-wavelength bands in the absorption spectra of the mentioned tautomers should depend closely on the solvent polarity. Thus, substantial changes to the position of the absorption bands that occur upon changing media are due to specific interactions of the tautomeric forms with the solvent. In view of these facts, the hydrazone tautomers should absorb at longer wavelength relative to that of the azo-enamine ones. Therefore, azo-enamine–hydrazone transformation should be accompanied by a bathochromic shift of the longer wavelength absorption band. In fact, compound **5** reflected such phenomena whereas the predicted spectra show an opposite behavior (Fig. 2, Tables 4 and 5).

Based on the electronic absorption transitions predicted for the tautomers investigated here (Table 5), in the visible region the hydrazone tautomers should show bands at 340–379 nm and the azo-enamine forms absorb strongly at 419–435 nm depending

Table 2
Physicochemical and structural parameters predicted in the gaseous phase at the PM6 (S_0 state) and PM6/CI (S_1 state) levels of theory.

Comp.	Form	$\Delta_{f,298}H^0$ (kcal/mol)	μ (D)	μ_{S_1} (D)	$\mu_{S_1} - \mu$ (D)	Energy		Θ
						HOMO	LUMO	
1	Azo	157.53 (229.34)	4.99	5.14	0.15	-9.20	-1.27	-144.18
	Hydrazone	145.91 (220.58)	4.37	4.99	0.62	-8.95	-1.15	174.39
	Azo-enamine	144.84 (204.20)	7.50	5.61	-1.89	-8.48	-1.40	-179.97
2	Azo	146.82 (198.45)	5.81	4.08	-1.73	-9.15	-1.15	-147.70
	Hydrazone	135.46 (211.43)	4.35	4.26	-0.09	-8.90	-1.06	174.04
	Azo-enamine	134.36 (194.64)	7.50	6.08	-1.42	-8.34	-1.32	-179.99
3	Azo	115.22 (169.24)	5.39	2.80	-2.59	-9.11	-1.10	-143.64
	Hydrazone	104.57 (180.81)	4.70	4.99	0.29	-8.88	-1.03	175.08
	Azo-enamine	103.22 (163.47)	5.89	4.90	-0.99	-8.26	-1.28	-179.85
4	Azo	72.08 (153.34)	3.87	5.03	1.16	-9.53	-1.33	-99.26
	Hydrazone	58.57 (130.93)	4.69	8.55	3.86	-9.13	-1.62	175.80
	Azo-enamine	56.47 (113.88)	7.55	5.89	-1.66	-8.74	-1.77	179.97
5	Azo	155.78 (237.15)	7.10	8.30	1.20	-9.64	-1.65	-99.17
	Hydrazone	142.82 (213.26)	7.58	13.23	5.65	-9.27	-1.99	176.42
	Azo-enamine	139.23 (201.61)	11.16	8.98	-2.18	-9.03	-1.81	179.93
6	Azo	149.94 (231.20)	3.93	4.97	1.04	-9.42	-1.37	-114.49
	Hydrazone	136.95 (212.22)	4.62	6.52	1.90	-9.05	-1.27	-174.04
	Azo-enamine	134.83 (193.13)	7.88	5.40	-2.48	-8.58	-1.56	-179.92
7	Azo	111.57 (164.43)	4.37	2.49	-1.88	-9.17	-1.23	-143.23
	Hydrazone	100.83 (175.70)	4.08	5.19	1.11	-8.95	-1.10	173.69
	Azo-enamine	99.28 (159.23)	5.99	4.22	-1.77	-8.39	-1.35	179.97

$\Delta_{f,298}H^0$ —enthalpy of formation in the S_0 and S_1 (in parentheses) states, μ , μ_{S_1} —dipole moments (Debye) in the S_0 and S_1 states respectively, Θ —dihedral angle between C₂C₁₀N₁₂N₁₃; HOMO and LUMO, in eV, indicate the energies of the highest occupied and lowest unoccupied molecular orbitals.

Table 3Enthalpies of formation (in kcal/mol) predicted at the PM6 (COSMO) (S_0 state) and PM6/CI (COSMO) (S_1 state) levels of theory.

Comp.	Form	Medium					
		C ₂ H ₅ OH	DMSO	DMF	CH ₃ CN	CH ₂ Cl ₂	CHCl ₃
1	Azo	146.46 (228.24)	146.12 (229.59)	146.17 (227.97)	146.19 (227.99)	147.87 (230.11)	149.46 (232.11)
	Hydrazone	131.16 (202.87)	130.49 (222.10)	154.46 ^a (209.66)	130.75 (202.14)	133.07 (205.09)	135.42 (209.51)
	Azo-enamine	130.03 (195.69)	129.35 (194.17)	146.14 (192.94)	129.64 (194.49)	132.18 (193.45)	134.45 (198.47)
	Ionized form	33.08 ^a (104.67)	124.66 (154.13)	125.27 (154.68)	125.31 (154.69)		
2	Azo	135.20 (226.67)	134.91 (223.80)	134.90 (225.88)	134.91 (226.82)	136.59 (221.51)	138.31 (220.69)
	Hydrazone	120.89 (221.45)	120.18 (203.26)	144.92 ^a (206.25)	120.43 (203.56)	122.93 (204.81)	125.37 (204.67)
	Azo-enamine	119.44 (183.95)	118.67 (183.16)	136.60 (181.95)	118.98 (183.50)	121.56 (186.14)	123.91 (188.67)
	Ionized form	19.74 (103.17)	17.74 (101.57)	18.34 (102.41)	18.40 (102.05)		
3	azo	101.66 (191.70)	101.15 (191.36)	101.31 (192.33)	101.33 (191.84)	103.26 (191.15)	105.15 (190.84)
	Hydrazone	89.48 (155.90)	88.89 (154.96)	89.05 (155.19)	89.05 (155.34)	91.48 (158.73)	93.94 (161.72)
	Azo-enamine	86.31 (147.20)	85.91 (146.85)	85.86 (146.77)	85.88 (146.78)	88.37 (149.20)	90.88 (151.75)
	Ionized form	-13.41 (69.82)	-15.47 (67.67)	-14.88 (68.67)	-14.75 (68.90)		
4	Azo	53.44 (109.59)	52.77 (108.73)	53.00 (109.17)	52.81 (134.79 ^a)	55.47 (111.54)	58.01 (115.20)
	Hydrazone	38.34 (107.65)	37.67 (107.02)	37.85 (107.24)	37.85 (107.31)	40.59 (110.07)	43.36 (112.88)
	Azo-enamine	35.27 (103.63)	34.42 (102.79)	34.68 (103.07)	34.69 (103.17)	37.93 (106.78)	41.21 (109.62)
	Ionized form	-66.94 (10.15)	-67.33 (10.23)	-66.78 (10.60)	-66.70 (10.67)		
5	Azo	137.40 (201.68)	136.82 (202.87)	136.96 (202.38)	136.97 (202.51)	139.48 (208.64)	142.05 (224.93)
	Hydrazone	122.08 (190.93)	121.45 (189.59)	121.55 (190.11)	121.57 (190.14)	124.39 (193.57)	127.17 (196.06)
	Azo-enamine	119.09 (182.77)	118.25 (182.24)	118.46 (182.42)	118.48 (182.38)	121.30 (191.80)	125.25 (186.76)
	Ionized form	17.88 (65.72)	15.99 (63.68)	16.53 (64.16)	16.59 (64.27)		
6	Azo	136.99 (218.63)	136.63 (204.50)	136.74 (204.04)	136.72 (218.28)	138.28 (220.42)	139.93 (194.64)
	Hydrazone	122.42 (206.20)	121.73 (205.51)	121.63 (205.73)	121.95 (205.69)	124.50 (208.17)	126.91 (210.09)
	Azo-enamine	119.90 (184.81)	119.24 (184.15)	119.44 (184.38)	119.45 (184.37)	122.05 (184.95)	124.37 (189.36)
	Ionized form	19.50 (102.51)	17.63 (101.33)	18.19 (101.75)	18.23 (101.88)		
7	Azo	96.86 (189.35)	96.09 (188.61)	96.49 (189.02)	96.50 (189.03)	98.66 (190.68)	100.63 (192.16)
	Hydrazone	82.70 (165.80)	81.93 (165.07)	82.14 (165.23)	82.17 (165.19)	85.34 (168.28)	88.12 (170.77)
	Azo-enamine	81.21 (154.24 ^a)	80.31 (144.31)	80.60 (144.62)	80.69 (144.72)	83.56 (147.68)	86.36 (150.66)
	Monoanionic form	-18.49 (62.78)	-20.60 (62.58)	-20.04 (62.96)	-19.98 (62.94)		
	Dianionic form	-100.14 (-40.83)	-105.30 (-45.64)	-103.81 (-44.28)	-103.69 (-44.17)		

^a These inharmonic values have been checked several and were also tested by PM3 and the same tendency has been found.

on the substituents (R). Besides, many weaker transitions can be expected for the azo-enamine tautomers in the range of 300 nm and for the hydrazone forms between 250 and 280 nm. The results given in Table 5, the calculations – based on AM1 geometries – predicted a very small intensity (*f*) for the longest wavelength transition bands in the case of the azo tautomers compared to $\pi-\pi^*$ one within the heterocyclic moiety. In the hydrazone, azo-enamine tautomers with acceptor substituents predicted to absorb light at longer wavelength compared to derivatives with donor substituents. Consequently, positive solvatochromism of the visible band should be noted on transferring from very strong donor substituents to poor acceptor ones. Generally, the above findings are in consistent with the experimental UV–vis spectra to some extent and the slight deviation may in part be due to the solvation effects (Table 4). Further information provides values of energies of the first HOMO and LUMO orbitals showing that the difference between HOMO and LUMO depends markedly on the substituents (Table 2).

3.2. Electronic absorption spectra in ethanol

The values of λ_{\max} and the excitation coefficients ($\log \epsilon$) of the characteristic absorption bands of the dyes **1–7** in various organic solvents are listed in Table 4. Only the longer wavelength absorption bands are tabulated as the shorter wavelength band remained virtually unaltered in different solvents. Fig. 3 represents the absorption spectra of the studied compounds (**1–7**) in ethanol. The bands observed in the range 205–265 nm are due to $\pi-\pi^*$ transitions within the π -electronic system of the heterocyclic moiety.

This assignment is in accordance with the literature data and it is sustained by the slight effect on these transitions by the nature of the substituent on the phenyl ring [31,39]. The weak band appeared at around 300 nm can be attributed to $n-\pi^*$ of the $-N=N-$ linkage. Evidence supporting this assignment comes from the disappearance of this band in the acidic medium. Obviously, the main band in all compounds investigated appears in the range 400–425 nm with a maximum absorption (λ_{\max}) depending largely on their molecular structure. This band can be regarded as a $\pi-\pi^*$ transition involving the π -electronic system throughout the whole molecule with a considerable charge transfer (CT) character. This CT originates mainly from the aryl moiety as a donor to the heterocyclic benzothiazole ring [31,40,41]. The CT nature of this band is achieved from its broadness [42], the sensitivity of its λ_{\max} to the type of the substituent attached to the phenyl and the nature of the solvent (Table 4 and Fig. 3). Generally, it acquires blue shift in its λ_{\max} when R is an electron acceptor group whereas an electron releasing substituent results in a red shift (Table 4). This behavior in compounds **2**, **3**, and **7** can be interpreted on the basis of the expected low excitation energy for the intramolecular CT band. This is a result of the increased delocalization of the π -electronic system relative to the former ones. The discrepancy of compound **5** from this trend can be explained either by the antagonizing effect by the nitro group or under the acceptor character of this group and consequently the CT transitions may take place in the opposite direction [26].

In particular, compound **5** exhibits a special behavior that is a new band at longer wavelength (525 nm) has appeared. This extra visible band exceeds by far the polarity effect of the solvent and could be attributed to the absorption by the ionized form even

Table 4
Experimental electronic absorption spectral data of compounds 1–7.

Compound	C ₂ H ₅ OH		CH ₃ OH		DMF		DMSO		CH ₃ CN		Acetone		CH ₂ Cl ₂		CHCl ₃		CCl ₄	
	λ_{\max}	$\log \epsilon$	λ_{\max}	$\log \epsilon$	λ_{\max}	$\log \epsilon$	λ_{\max}	$\log \epsilon$	λ_{\max}	$\log \epsilon$	λ_{\max}	$\log \epsilon$	λ_{\max}	$\log \epsilon$	λ_{\max}	$\log \epsilon$	λ_{\max}	$\log \epsilon$
1	399	4.49	398	4.51	448	4.50	420	4.40	460 _{sh}	4.05	462 _{sh}	3.77	400	4.47	402	4.47	404	4.48
	231	4.89	218	4.47					404	4.40	399	3.78						
2	407	4.51	405	4.51	450	4.57	422	4.44	409	4.47	405	4.47	410	4.49	411	4.48	412	4.46
	232	4.89	233	4.89														
3	418	4.48	416	4.49	452	4.60	445	4.48	424	4.47	417	4.48	421	4.47	422	4.48	424	4.42
	301	3.83	301	3.86														
	232	4.90	232	4.89														
4	402	4.56	400	4.59	480	4.73	481	4.50	467	4.17	475	3.70	401	4.49	403	4.57	404	4.55
	271	4.20	265	4.23	392 _{sh}	3.94	412	4.34	400	4.46	399	4.54						
	209	4.53	215	4.65														
5	525	3.68	519	4.03	548	4.76	552	4.52	539	4.47	543	4.11						
	418 _{sh}	4.54	418 _{sh}	4.52	375	3.80	420	4.25	419	4.28	418 _{sh}	4.54	421	4.61	420	4.60	418 _{sh}	4.58
	406	4.57	406	4.54					405	4.30	406	4.40	409	4.66	410	4.63	407	4.62
	301	3.68	298	3.92														
	211	4.52	213	4.56														
6	399	4.46	398	4.48	456	4.58	450	4.39	457	4.23	465 _{sh}	3.68	402	4.45	404	4.46	405	4.45
	301	3.72	299	3.76					408	4.37	399	4.45						
	249	4.11	249	4.14														
	224	4.28	223	4.33														
	205	4.22	206	4.25														
7	423	4.41	420	4.44	450	4.52	435	4.44	425	4.42	425	4.45	424	4.46	425	4.44	425	4.42
	308 _{sh}	3.76	308 _{sh}	3.77														
	264	4.06	262	4.09														
	212	4.64	218	4.74														

λ_{\max} —position of band maxima in absorption spectra (nm), ϵ —absorption coefficients ($M^{-1} cm^{-1}$) and sh—shoulder.

though the basicity character of ethanol is quite low. This finding occurs on the basis of the well-known acid–base equilibrium ($HA + S \rightleftharpoons A^- + HS^+$) of other azo dyes which was discovered by an examination of their absorption spectra [28,43]. Such phenomenon is much more pronounced in this derivative due to the presence of the nitro group (a very strong electron withdrawing group). Consequently, the introduction of strongly acceptor group at C₁₇

in the phenyl moiety facilitates the deprotonation process. Additionally, we have to state here that the spectra of this dye in all solvents except DMF and DMSO contain elements characteristic of both hydrazone and azo-enamine forms (Scheme 1, Fig. 2). Such tautomerization ability is demonstrated by the composite nature of the main visible band, where a clear shoulder can be observed in the longer wavelength side. Therefore, it is possible to assign

Table 5
Wavelengths (nm) and oscillator strengths (in parentheses) of electronic absorption transitions predicted in gaseous phase at AM1/CI level of theory.

Form	Compound						
	1	2	3	4	5	6	7
Azo	353(0.06)	352(0.06)	352(0.06)	352(0.06)	351(0.06)	352(0.06)	352(0.06)
	295(0.12)	305(0.20)	324(0.06)	298(0.13)	300(0.13)	304(0.18)	326(0.10)
	264(0.11)	264(0.10)	310(0.22)	247(0.88)	257(0.14)	262(0.08)	315(0.24)
	249(0.95)	289(0.95)	263(0.10)	224(0.24)	245(1.08)	251(0.10)	264(0.10)
	228(0.24)	229(0.30)	249(0.89)	215(0.42)	226(0.30)	248(0.93)	249(0.92)
	215(0.73)	215(0.81)	218(0.84)	211(1.20)	211(0.77)	214(0.91)	231(0.28)
Hydrazone	352(0.06)	375(0.81)	347(0.56)	341(0.43)	344(0.48)	344(0.53)	379(0.83)
	332(0.30)	356(0.76)	293(0.09)	275(0.32)	272(0.40)	321(0.08)	356(0.07)
	317(0.13)	280(0.37)	279(0.07)	260(0.14)	267(0.07)	286(0.32)	283(0.36)
	280(0.12)	270(0.78)	273(0.20)	243(0.25)	255(0.10)	266(0.11)	270(0.08)
	270(0.31)	247(0.17)	246(0.23)	233(0.09)	241(0.39)	241(0.28)	247(0.19)
	265(0.12)	228(0.62)	222(0.25)	228(0.09)	230(0.22)	225(0.19)	229(0.45)
	244(0.29)	219(0.25)	220(0.31)	221(0.17)	227(0.13)	220(0.24)	219(0.24)
	218(0.28)	213(0.55)	215(0.19)	218(0.42)	216(0.29)	215(0.43)	214(0.46)
	215(0.68)	207(0.39)	208(0.23)	213(0.70)	209(0.50)	210(0.37)	209(0.47)
	Azo-enamine	419(0.97)	424(1.01)	426(1.04)	428(1.04)	435(1.08)	426(1.02)
264(0.22)		305(0.18)	309(0.11)	306(0.14)	301(0.10)	307(0.11)	309(0.11)
260(0.31)		261(0.37)	262(0.32)	262(0.49)	262(0.44)	262(0.43)	262(0.38)
249(0.31)		249(0.30)	249(0.30)	247(0.28)	246(0.29)	248(0.30)	249(0.30)
233(0.12)		234(0.16)	235(0.20)	233(0.16)	234(0.22)	234(0.16)	235(0.20)
217(0.49)		219(0.51)	220(0.56)	225(0.31)	229(0.28)	229(0.21)	220(0.53)
207(0.47)		209(0.39)	209(0.40)	205(0.97)	208(0.53)	209(0.25)	209(0.37)

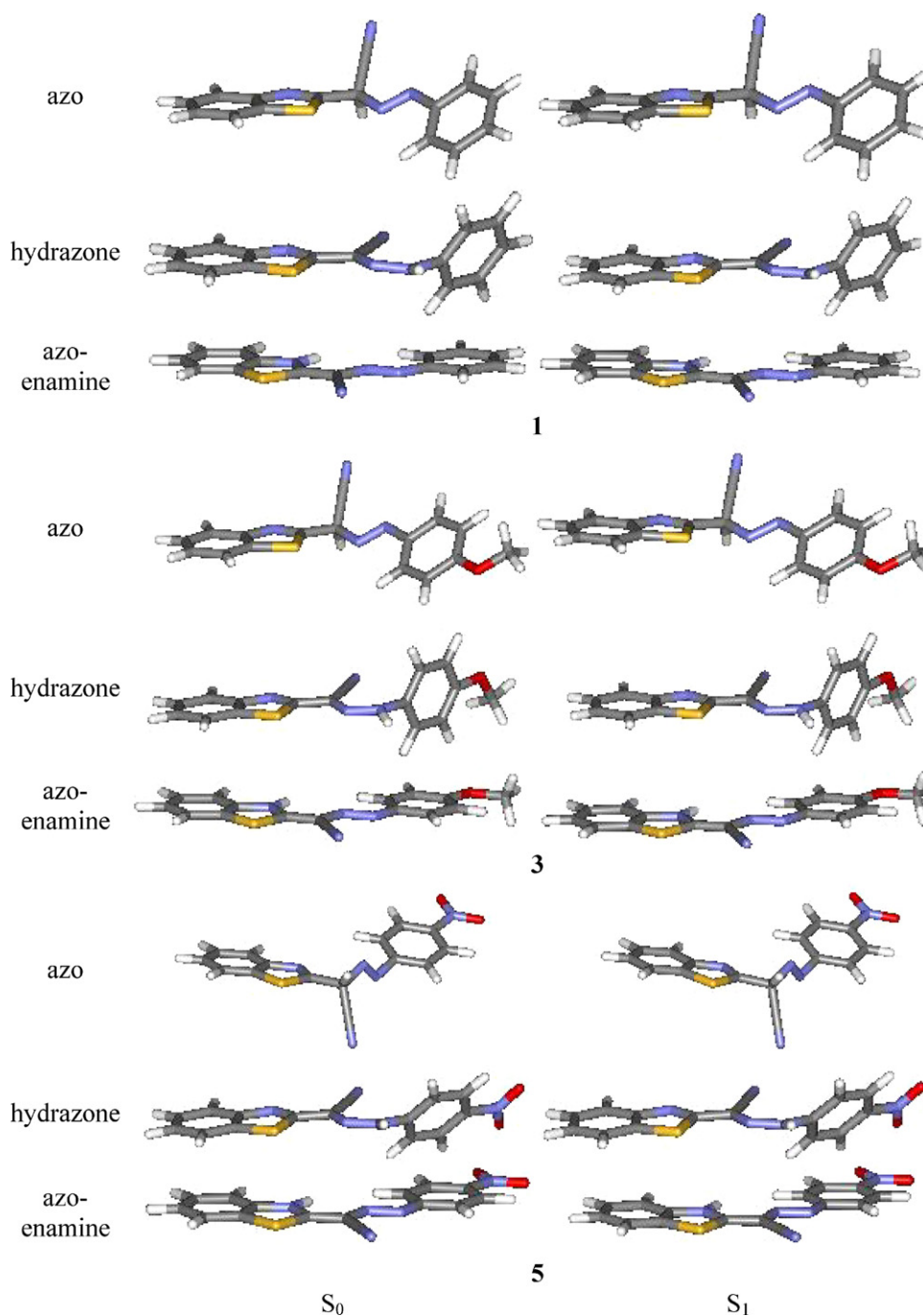


Fig. 1. The PM6 optimized structures of the tautomers of compounds 1, 3 and 5 in ground (S_0) and excited state (S_1) as a representative example (Scheme 1).

the shorter wavelength band to a transition within the hydrazone form, while the longer band to a similar transition within the azo-enamine tautomer. Similar acid–base equilibrium is also recognized in the other derivatives and it might be responsible for the disappearance of the prototropic equilibrium in these compounds. Since the tautomeric equilibrium should be influenced by the possibility of interaction with the solvent through charge transfer from solute to solvent. This effect, however, could not enable us to see different forms in the other investigated compounds. Detailed study of the tautomerism in these compounds may provide interesting information. Examination of this problem was not the main target of the present piece of work.

3.3. Effect of solvents and acid–base equilibrium

The electronic absorption spectra of compounds 1–7 were studied in organic solvents with different polarities to investigate their solvatochromic behavior. Comparison of absorption maxima of the dyes investigated revealed a blue shift in λ_{\max} of the main visible band as the polarity of the solvent increases. This shift can be explained on the basis that the excited states of these dyes are less polar than the ground states. As a consequence, the non-polar solvents stabilize these dyes more than polar ones and this result is generally very close to the calculated dipole moments for azo-enamine form (Table 2).

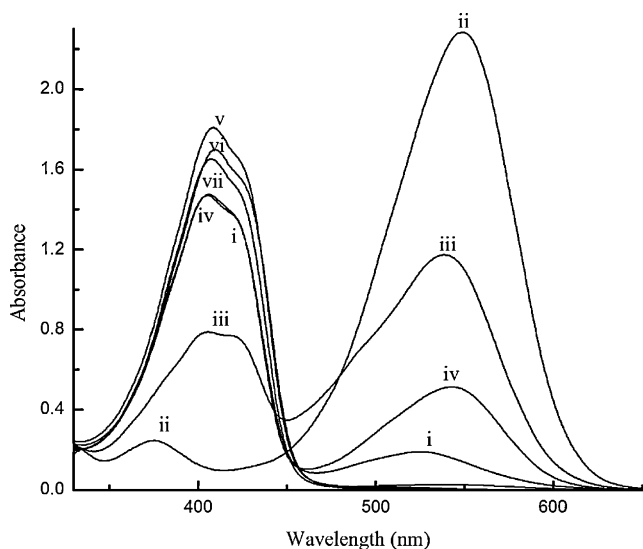


Fig. 2. Absorption spectra of 4.0×10^{-5} M solution of compound **5** ($p\text{-NO}_2$) in organic solvents. EtOH (i); DMF (ii); acetonitrile (iii); acetone (iv); CH_2Cl_2 (v); CHCl_3 (vi) and CCl_4 (vii).

Moreover, our results demonstrate that compounds **1–3** and **6, 7** exist principally in the ionized form in DMSO and DMF due to their low ionization potential and high hydrogen bond accepting character [44]. Moreover, the spectra of compounds **4** and **5** indicate that they coexist in acid–base equilibrium, (representative Fig. 2). Furthermore, dissolving compounds **1** and **6** in acetone and acetonitrile showed a clear shoulder at a longer wavelength. This finding makes one also propose without any doubt that different structures are involved in equilibrium. Thus, it is possible to assign the shorter wavelength visible band displayed by the neutral form HA in compounds **1** and **4–6** to an intramolecular CT within the azo-enamine and/or hydrazone forms of the molecule. While the longer wavelength visible one can be attributed to a similar transition within anionic form (A^-). It is anticipated that the CT interaction occurs more easily for the A^- form than the HA one. It is of considerable interest to emphasize that the appearance of the absorption band due to the ionized form in the polar solvents is because of the high basicity (pKs) of these solvents compared to the non-polar ones [44,45]. Strong evidence verifying such equilib-

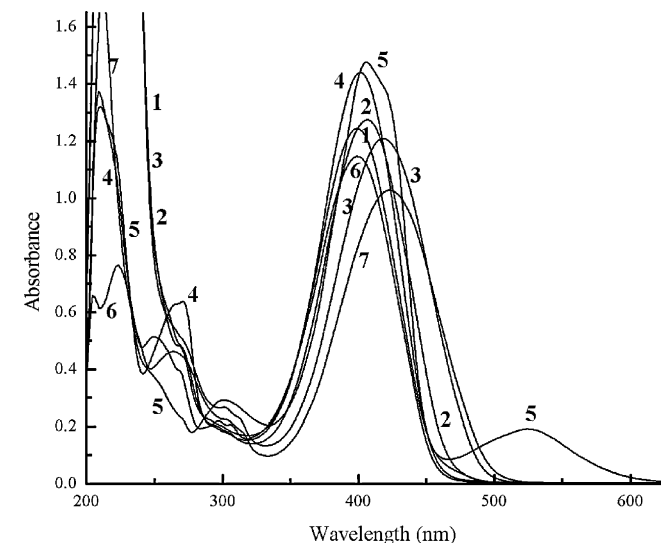


Fig. 3. Electronic absorption spectra of 4.0×10^{-5} M solution of compounds **1–7** in ethanol.

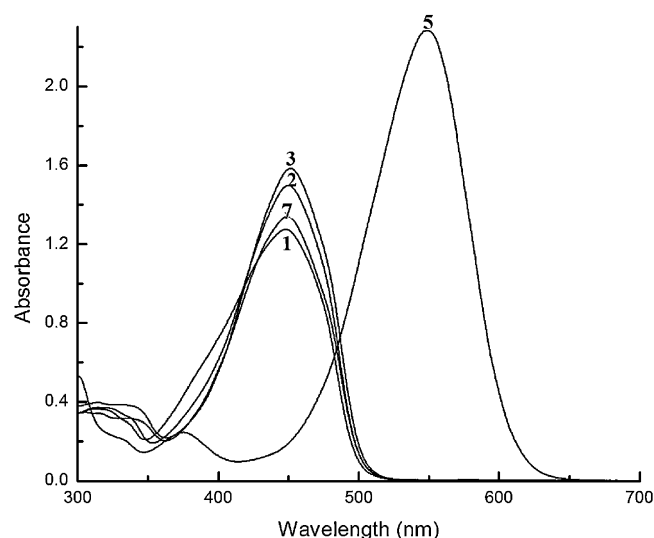


Fig. 4. Visible absorption spectra of 4.0×10^{-5} M solution of compounds **1–3, 5** and **7** in DMF.

rium in the polar solvents is obtained from two important features namely:

The position of λ_{max} of a solution containing few drops of 1.0N NaOH is the same as in pure organic solvents, while in a solution containing 1.0N HCl only the shorter wavelength band appears.

The color of the dye solution containing NaOH is exactly the same as in pure solvents and widely different from that in solvents containing HCl.

Also it is markedly clear that the electron donating nature contributes to the stabilization of the neutral form and hence the above equilibrium has not been observed in compounds **2, 3** and **7**.

3.4. Spectra in mixed organic solvents

The visible spectra of compounds **1–3, 5** and **7** in DMF– CCl_4 , DMF– CHCl_3 , DMF–acetone and DMF– $\text{C}_2\text{H}_5\text{OH}$ binary solvent mixtures were undertaken to obtain an insight into the origin of the interaction between these dyes and DMF. This is performed to find

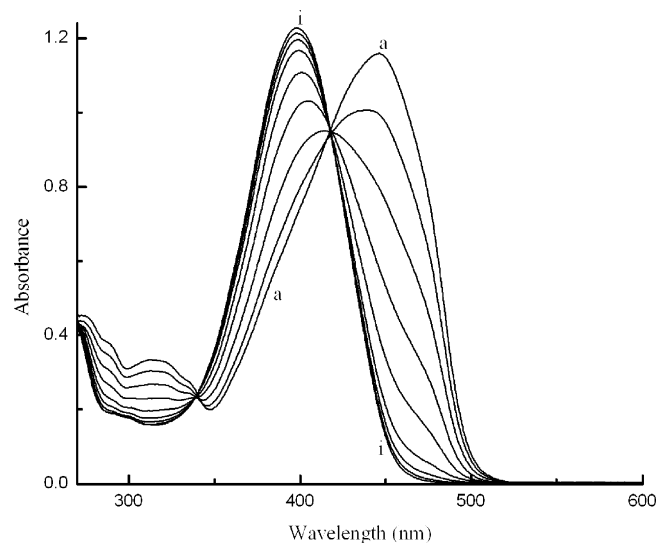


Fig. 5. Visible spectra of 4.0×10^{-5} M solution of compound **1** ($p\text{-H}$) in DMF–EtOH mixture solvents. (a) 1.30 M DMF; (b) 2.59 M DMF; (c) 3.89 M DMF; (d) 5.19 M DMF; (e) 6.49 M DMF; (f) 7.78 M DMF; (g) 9.08 M DMF; (h) 10.38 M DMF and (i) 11.67 M DMF.

Table 6Values of K_{ion} and $-\Delta G$ for the ionization process for some azo derivatives from the investigated compounds.

System	Compound									
	1		2		3		5		7	
	K_{ion}	$-\Delta G$								
DMF–acetone	5.13	0.97	6.03	1.07	5.13	0.96	4.57	0.90	5.75	1.03
DMF–C ₂ H ₅ OH	8.13	1.24	8.91	1.30	7.94	1.23	3.89	0.80	8.32	1.25
DMF–CHCl ₃	8.51	1.26	9.55	1.33	9.77	1.35	6.03	1.06	10.00	1.36
DMF–CCl ₄	6.76	1.13	8.32	1.25	9.12	1.30	4.68	0.91	12.30	1.49

how these derivatives, dissolved in highly proton acceptor (DMF), would respond to the presence of successfully increasing amounts of CCl₄, CHCl₃, acetone and ethanol. It is evident that in pure DMF the dyes exhibit only one band in the visible region at wavelengths depending upon the molecular structure (Table 4, Fig. 4). When the second solvent is added into the solution of the dye in dimethyleformamide, the band which previously assigned to the absorption by the ionized form is shifted to a lower wavelength. With the increase of the mole fraction of the added solvent to the binary solvent mixture, the absorption band by neutral form develops gradually and keeps almost constant at very low amount of DMF. The spectra recorded in all mixed solvents show a fine isosbestic point which indicates the establishment of equilibrium between the ionized and non-ionized forms of the molecule (Fig. 5). This behavior also

indicates that DMF molecules have a greater tendency to form ionized forms with the solute molecules comparable to acetone and ethanol. The value of the ionization constant (K_{ion}) was determined from the variation of absorbance obtained by decreasing the DMF concentration at a constant wavelength using the following equation [46].

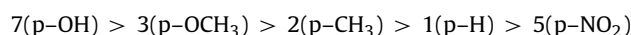
$$\text{Log } C_{\text{DMF}} = \log K_{\text{ion}} + \log \left(\frac{A - A_{\text{min}}}{A_{\text{max}} - A} \right) \quad (1)$$

where A_{min} , absorbance in a low polarity solvent; A_{max} absorbance in a high polarity solvent (DMF); A absorbance in the mixed solvent.

Gibbs free energy (ΔG) values are obtained by applying Eq. (2):

$$-\Delta G = RT \ln K_{\text{ion}} \quad (2)$$

The values of ΔG and K_{ion} of the ionization equilibrium existing in solution are cited in Table 6. The negative values of the free energy change of the ionization process indicate that this process is spontaneous. In general, the experimental results presented in Table 6 show that the values of K_{ion} and ΔG of the compounds investigated in mixed solvent are dependent upon the substituents and increase in the following sequence:



This order is in harmony with the increase in the donating character of the substituent.

3.5. Time effect

The most striking behavior in these compounds is the visible spectrum of compound 7 in DMF where the main band with λ_{max} at 450 nm varies apparently with time. This can be considered as further evidence that this band corresponds to an association process through a solute–solvent interaction. The two possible mono- and dianionic structures exhibit low thermodynamic values in both the ground and excited electronic states (Table 3). Accordingly, both mono- and dianionic forms of 7 can exist in DMF. As can be readily seen from Fig. 6, the intensity of the former band (due to absorption by dianionic form) decays gradually with time, while a shorter wavelength visible band ($\lambda_{\text{max}} = 397$) starts to appear as a shoulder and its absorbance increases gradually. After a long time the extinction of the shorter wavelength band becomes higher and the longer wavelength band completely disappears. This behavior denotes that the rate of dissociation – the concentration of the equilibrium $\text{HA}^- + \text{S} \rightleftharpoons \text{A}^{2-} + \text{HS}^+$ – shifted predominantly toward the backward direction in such equilibrium. This confirms the existence of the compound in acid–base equilibrium and supports our previous discussion.

4. Conclusion

We have investigated solvatochromism, acid–base equilibrium, preferred tautomers of seven azo compounds using UV–vis spectra and quantum–mechanical calculations at the semiempirical levels (AM1 and PM6). Our calculated results give rise to the following findings:

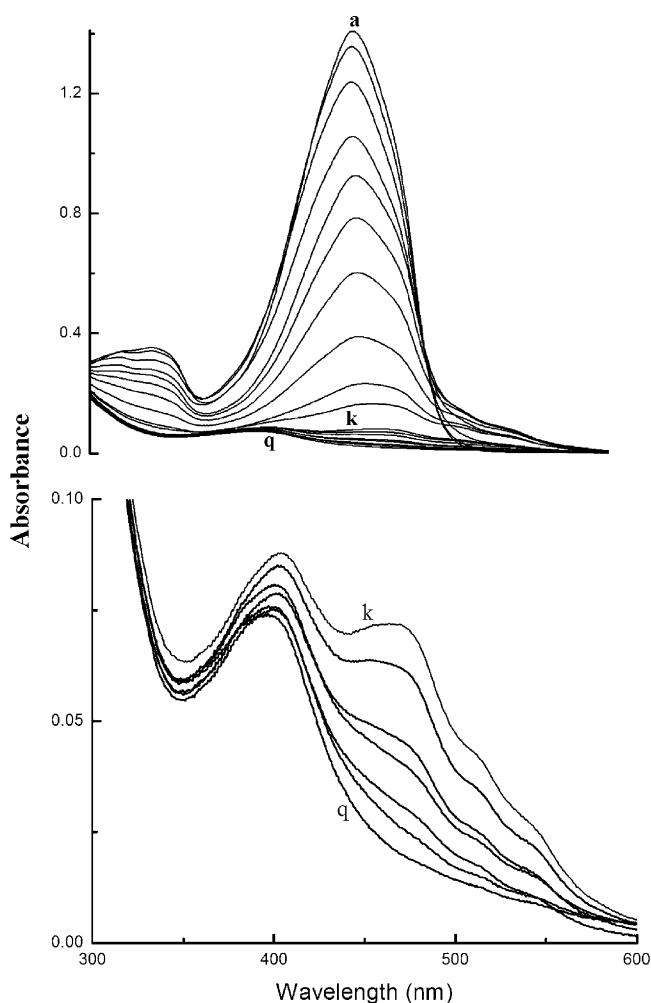


Fig. 6. Time effect of 4.0×10^{-5} M solution of compound 7 in DMF at (a) 1 h; (b) 48 h; (c) 96 h; (d) 216 h; (e) 288 h; (f) 360 h; (g) 432 h; (h) 528 h; (i) 624 h; (j) 744 h; (k) 816 h; (l) 936 h; (m) 984 h; (n) 1056 h; (o) 1176 h; (p) 1272 h and (q) 1368 h.

- Two of the plausible tautomers – azo and hydrazone – are essentially non-planar in the ground and excited electronic states.
- The azo tautomers are characterized by higher values of ΔH_f which means that compounds **1–7** are not likely to exist.
- The predicted electronic absorption spectra have some considerable shifts compared to the experimental spectral data.

The role of substituents and influence of solvents on the UV–vis spectra are noticeable. The occurrence of an intermolecular CT transition in all compounds in DMF as a solvent is quite reasonable in view of:

- The well-known strong hydrogen bond acceptor character of DMF.
- Its low ionization potential (9.12 eV) [44,45].

Nevertheless, recent crystallographic data concerning compound **2** showed that hydrazone tautomer is preferred [47]. However, our theoretical and experimental results reveal that azo-enamine and hydrazone tautomers as well as anionic forms are energetically favored. Compound **7** is considerably affected by time.

Further investigation is under study including NMR studies of these compounds as well as the calculation of their equilibrium constants in different media for further insight into their tautomerization ability. The role of the medium on the acidity constants will also be studied.

Acknowledgment

We are bottomless grateful to M.F. Aly professor of organic chemistry, South Valley University for his limitless help and fruitful discussions.

References

- [1] D.A. Skoog, D.M. West, F.J. Holler, *Fundamental of Analytical Chemistry*, 6th ed., Saunders College Publishing, 1992, p. 561.
- [2] D.L. Rodman, N.A. Carrington, H. Qiu, K. Goswami, Z.L. Xue, *Anal. Chem. Acta* 548 (2005) 143–147.
- [3] G.D. Christian, *Analytical Chemistry*, 5th ed., John Wiley and Sons, New York, 1994, p. 398.
- [4] H.W. Gao, X.H. Liu, Z. Qiu, L. Tan, *Amino Acids* 36 (2) (2009) 251–260.
- [5] F. Karci, N. Sener, M. Yamac, I. Sener, A. Demirçali, *Dyes Pigments* 80 (2009) 47–52.
- [6] M. Perez, M.D. Part, J.L. Beltran, *J. Chromatogr. A* 871 (2000) 227–234.
- [7] A. Natansohn (Ed.), *Azobenzene-Containing Materials*, Wiley-VCH Weinheim, 1999.
- [8] Y. Cheng, M. Zhang, H. Yang, F. Li, T. Yi, C. Huang, *Dyes Pigments* 76 (2008) 775–783.
- [9] Y.F. Cheng, D.T. Zhao, M. Zhang, Z.Q. Liu, Y.F. Zhou, T.M. Shu, F.Y. Li, T. Yi, C.H. Huang, *Tetrahedron Lett.* 47 (2006) 6413–6416.
- [10] A. Pandey, P. Singh, L. Iyengar, *Inter. Biodet. Biodeg.* 59 (2007) 73–84.
- [11] H. Kocaokutgen, S. Özkinali, *Dyes Pigments* 63 (2004) 83–88.
- [12] P. Rajaguru, L. Vidy, B. Baskarasethupathi, P.A. Kumar, M. Palanivel, K. Kalaiselvi, *Mutat. Res.* 517 (2002) 29–37.
- [13] G.A. Umbuzeiro, H. Freeman, S.H. Warren, D.P. Oliveira, Y. Terao, T. Watanabe, L.D. Claxton, *Chemosphere* 60 (2005) 55–64.
- [14] T.S. Gore, B.S. Joshi, S.V. Synthakar, B.D. Tilak (Eds.), *Recent Progress in the Chemistry of Natural and Synthetic Coloring Matter*, Academic Press, New York, 1962.
- [15] D.M. Sturmer, in: A. Weissberger, E.C. Taylor (Eds.), *Special Topics in Heterocyclic Chemistry*, Wiley, New York, 1977.
- [16] A.D. Towns, *Dyes Pigments* 42 (1999) 3–28.
- [17] A.E.H. Machado, N.M.B. Neto, L.T. Ueno, L.F. de Paula, D.M.S. Araujo, G.S. Oliveira, W.R. Gomes, R. de Paula, P.L. Franzen, S.C. Zilio, A.M.F. Oliveira-Campos, A.M. Fonseca, L.M. Rodrigues, P.O. Nkeonye, R. Hrdina, J. Photochem. Photobiol. A: Chem. 199 (2008) 23–33.
- [18] A. Schmidt, E. Bach, E. Schollmeyer, *Dyes Pigments* 56 (2003) 27–35.
- [19] A. Emandi, I. Serban, R. Bandula, *Dyes Pigments* 41 (1999) 63–77.
- [20] N.M. Rageh, *Spectrochim. Acta A* 60 (2004) 103–109.
- [21] E. Buncel, S. Rajagopal, *J. Org. Chem.* 54 (1989) 798–809.
- [22] P.A. Lefevre, H. Tinwell, J. Ashby, *Mutagenesis* 12 (1) (1997) 45–47.
- [23] T.Yu. Ogul'chanskaya, V.M. Yashchuka, M.Yu. Losytskiya, I.O. Kocheshev, S.M. Yarmoluk, *Spectrochim. Acta A* 56 (4) (2000) 805–814.
- [24] A. Kamal, M.N. Khan, K.S. Reddy, Y.V.V. Srikanth, B. Sridhar, *Chem. Biol. Drug Des.* 71 (1) (2008) 78–86.
- [25] A.C. Razus, L. Birzan, N.M. Surugiu, A.C. Corbu, F. Chiraleu, *Dyes Pigments* 74 (2007) 26–33.
- [26] N.M. Rageh, A.A. Mohamed, H.M.S. Elkashaf, S.A. Ibrahim, Y.H. Ebead, *Can. J. Spectrosc.* 43 (1999) 176–181.
- [27] M.R. Mahmoud, S.A. Ibrahim, M.A. Hamed, *Spectrochim. Acta* 39 (1983) 729–733.
- [28] A.M. Hammam, N.M. Rageh, S.A. Ibrahim, *Dyes Pigments* 35 (1997) 289–296.
- [29] Y. Ebead, A.D. Roshal, A. Wroblewska, A.O. Doroshenko, J. Blazejowski, *Spectrochim. Acta A* 66 (2007) 1016–1023.
- [30] S.M. Rida, F.A. Ashour, S.A.M. El-Hawash, M.M. ElSemary, M.H. Badr, M.A. Shalaby, *Eur. J. Med. Chem.* 40 (2005) 949–959.
- [31] R.G. Dubenko, I.M. Bazavova, E.F. Gorbenko, *Zh. Org. Khim.* 20 (3) (1984) 577–583 [English Translation 523–528].
- [32] K. Saito, S. Kambe, Y. Nakano, A. Sakurai, H. Midorikawa, *Synthesis* (1983) 210–212.
- [33] J.J.P. Stewart, *J. Mol. Model.* 13 (2007) 1173–1213.
- [34] J.J.P. Stewart, *J. Comput. Chem.* 10 (1989) 209–220.
- [35] MOPAC2007, J.J.P. Stewart, *Stewart Computational Chemistry*, Version 8.301W web: <http://OpenMOPAC.net>.
- [36] M.J.S. Dewar, E.G. Zoebisch, F.F. Healey, J.J.P. Stewart, *J. Am. Chem. Soc.* 107 (1985) 3902–3909.
- [37] A. Alparone, V. Librando, *J. Mol. Struct., (Theorm)* 894 (2009) 128.
- [38] J.J.P. Stewart, *J. Mol. Model.* 14 (2008) 499–535.
- [39] A.R. Katritzky, *Physical Methods in Chemistry of Heterocyclic Compounds* [Russian Translation], Khimiya, Moscow-Leningrad, 1966, p. 371.
- [40] S. Wang, S. Shen, H. Xu, *Dyes Pigment* 44 (2000) 195–198.
- [41] M. Wang, K. Funabiki, M. Matsui, *Dyes Pigment* 57 (2003) 77–86.
- [42] G. Briegleb, *Electron Donor–Acceptor Complex*, Springer Verlag, Berlin, 1961.
- [43] N. Ertan, F. Eyduran, *Dyes Pigment* 27 (1995) 313–320.
- [44] C. Reichardt, *Solvents and Solvent Effects in Organic Chemistry*, 2nd ed., VCH, Weinheim, 1990, p. 432.
- [45] J.F. Coetzee, C.D. Ritchie, *Solute Solvent Interactions*, Marcel Dekker, New York, 1969, pp. 94.
- [46] R.M. Issa, M.M. Ghoneim, K.A. Idriiss, A.A. Harfouch, *Z. Phys. Chem. (F.M)* 94 (1975) 135–146.
- [47] K.O. Badahdah, *Heterocycles* 75 (2008) 1623–1630.